

Measurement report: Investigation of Optical Properties of Carbonaceous Aerosols from the Combustion of Different Fuels by an Atmospheric Simulation Chamber

5 Silvia G. Danelli¹, Lorenzo Caponi¹, Marco Brunoldi^{2,3}, Matilde De Camillis¹, Dario Massabò^{2,3}, Federico Mazzei^{2,3}, Tommaso Isolabella^{2,3}, Annalisa Pascarella^{4,5}, Paolo Prati^{2,3}, Matteo Santostefano¹, Francesca Tarchino⁶, Virginia Vernocchi², Paolo Brotto¹

¹PM_TEN Srl, Genoa, 16123, Italy

²INFN, Genoa Section, Genoa, 16146, Italy

³Department of Physics, University of Genoa, Genoa, 16146, Italy

10 ⁴BEES Srl, Genoa, 16121, Italy

⁵Istituto for the Application of Calculus (IAC) – CNR, Rome, 00185, Italy

⁶SIGE Srl, Genoa, 16161, Italy

Correspondence to: Federico Mazzei (federico.mazzei@ge.infn.it)

15 **Abstract.** This study investigates the optical properties and variability of the mass absorption coefficient (MAC) of carbonaceous aerosols produced by the combustion of different fuels. Emissions were also characterized in terms of particle size distribution and concentrations of elemental (EC) and organic carbon (OC). Experiments were conducted in an atmospheric simulation chamber with a soot generator fueled with propane and a commercial diesel engine running on regular diesel and Hydrotreated Vegetable Oil (HVO). Different methods of sampling and analyzing carbonaceous aerosols were
20 evaluated, focusing on workplace environments. The EC:TC (total carbon) ratios were found to be 0.7 ± 0.1 for propane, 0.15 ± 0.05 for diesel, and 0.4 ± 0.2 for HVO, indicating a higher proportion of OC in the diesel and HVO samples. Fresh soot particles showed monomodal log-normal distributions with peaks varying based on the fuel type and combustion process, with propane particles exhibiting a peak at larger particle sizes compared to HVO and diesel. The optical properties revealed that the MAC values varied across different fuel exhausts. Diesel combustion produced more light-absorbing particles compared
25 to propane and HVO, with MAC values measured between 870 and 635 nm ranging from 6.2 ± 0.5 to $9.4 \pm 0.4 \text{ m}^2 \text{ g}^{-1}$ for commercial diesel, 5.2 ± 0.5 to $7.8 \pm 1.1 \text{ m}^2 \text{ g}^{-1}$ for propane, and 5.8 ± 0.2 to $8.4 \pm 0.6 \text{ m}^2 \text{ g}^{-1}$ for HVO.

1 Introduction

Understanding of the processes involving carbonaceous aerosols, which constitute 20% to 50% of total aerosol mass in the atmosphere (Kanakidou et al., 2005; Putaud et al., 2010) is crucial for both climate and human health. Indeed, carbonaceous
30 aerosol produced during the incomplete combustion of biomass and fossil fuels significantly impact climate (Ackerman et al., 2000; Menon et al., 2002; Quinn et al., 2008; Ramanathan and Carmichael, 2008; Bond et al., 2013) and human health (Kanaya

et al., 2008, Sandrini et al., 2014, Pope et al., 2002; Anenberg et al., 2010; Gan et al., 2011; Cassee et al., 2013; Lelieveld et al., 2015).

The combustion-related absorbing particles are commonly referred to as black carbon (BC) when analyzed optically (Petzold et al., 2013) and as elemental carbon (EC) when characterized thermally (Bond and Bergstrom, 2006). Additionally, BC and EC often yield different concentration values (Massabò and Prati, 2021). Another important fraction of the by-product of combustion processes is organic carbon (OC). OC refers to the non-refractory fraction of carbonaceous aerosols, which can include numerous organic species. Among these, the light-absorbing species are known as Brown Carbon (BrC) (Moosmüller et al., 2009). The comparability of different thermal-optical protocols for OC and EC measurements (Cavalli et al., 2010, Giannoni et al., 2016) and the comparability of BC and EC measurements (Reisinger et al., 2008, Salako et al., 2012) remain active areas of research.

Soot particles, carbonaceous particles that are a by-product of the incomplete combustion of fossil fuels and/or biomass burning (Nordmann et al., 2013; Moore et al., 2014), are a significant component of anthropogenic particulate matter (PM), especially in urban areas, and are emitted by traffic, domestic stoves, industrial chimneys, and diesel engines (Weijers et al., 2011). Diesel engine exhaust, a complex mixture of gases, vapors, and fine particles, were classified in 2012 by the IARC as carcinogenic to humans (IARC category 1) and EC, a significant component of these emissions, is indicated as a common marker of exposure. For instance, Directive (EU) 2019/130, which amends Directive 2004/37/EC on the protection of workers from risks related to exposure to carcinogens or mutagens at work, sets binding occupational exposure limit values for diesel engine exhaust emissions at 0.05 mg m^{-3} , measured as EC. Lastly, the new Directive (EU) 2024/2881 on ambient air quality and cleaner air for Europe, incorporates the latest scientific evidence, including the updated WHO guidelines and, among various pollutants agents, it mandates the measurement of BC and EC in both rural and urban locations to support scientific understanding of their health and environmental impacts.

Understanding the properties and behavior of soot particles in the atmosphere, such as their spectral optical properties, is essential to fully assess their adverse effects and to properly define some of the methodologies used for their determination. The quantitative definition of the light absorbing properties of atmospheric aerosols is usually expressed by the mass absorption coefficient, MAC, which was first introduced by Putaud et al., 2010. MAC is the light absorption cross section normalized to the mass of a given species (e.g., EC/BC and/or BrC) of aerosol particles and it is given in units of ($\text{m}^2 \text{g}^{-1}$) and defined as

$$MAC(\lambda) = \frac{b_{abs}(\lambda)}{m}, \quad (1)$$

where $b_{abs}(\lambda)$, units of m^{-1} , is defined as the absorption coefficient at a specific wavelength and m is the mass concentration of the specific absorbing aerosol fraction.

Commonly accepted MAC values for freshly emitted BC are around $7.5 \pm 1.2 \text{ m}^2 \text{g}^{-1}$ at $\lambda = 550 \text{ nm}$ (Bond & Bergstrom 2006, Bond et al. 2013), with a recent study suggesting $8.0 \pm 0.7 \text{ m}^2 \text{g}^{-1}$ (Liu et al. 2019). However, atmospheric measurements show

a wide range of MAC values for BC-containing aerosols, from 5.5 to 45.9 m² g⁻¹ at $\lambda = 550$ nm and 4.2 to 19.9 m² g⁻¹ at $\lambda = 637$ nm (Genberg et al., 2013, Zanatta et al., 2016).

65 In this frame, we investigated the variability of MAC of carbonaceous aerosols produced under different fuel combustion conditions. Additionally, we evaluated and compared different methods of sampling and analyzing carbonaceous aerosols, with a particular focus on those used in workplace environments. Soot particles were collected using both an environmental monitoring sampler and personal air samplers, which are typically used to monitor workers' exposure to dust in various occupational settings. This selection reflects the increasing awareness and regulatory focus on the health impacts of diesel exhaust exposure in the workplace. An effective monitoring helps ensure compliance with environmental regulations and occupational safety standards and these samplers were included to cover all conditions and tools commonly employed for sampling carbonaceous aerosols in regulated environments. Indeed, this work is part of the CALIPSO project (Airborne Carbon: Limits, Impact, Protocols, and Operational Standards), funded by the Italy Liguria Region's PR FESR 2021–2027 program, which aims to evaluate and compare different methods of sampling and analysing carbonaceous aerosols, especially in workplaces.

75 Independent experiments were conducted inside an atmospheric simulation chamber (ASC) connected first to a soot generator and then a commercial diesel engine running on regular diesel and Hydrotreated Vegetable Oil (HVO). The use of an ASC allows for controlled, realistic environmental conditions, offering a compromise between laboratory and field experiments by providing quasi-realistic conditions without the variability of field measurements (Finlayson-Pitts and Pitts, 2000; Becker, 2006). Some examples of recent ASC applications studying the physicochemical and optical properties of different aerosol types are Caponi et al., 2017, Kumar et al., 2018, Hu et al., 2021 and Vernocchi et al. 2022.

2 Materials and methods

Experiments took place at the ChAMBRé (Chamber for Aerosol Modelling and Bio-aerosol Research) facility, located at the Physics Department of the University of Genoa and managed jointly with the Genoa Division of the National Institute of Nuclear Physics (INFN). ChAMBRé is a stainless-steel chamber, with a volume of about 2.2 m³. Temperature, pressure, and humidity, as well as the gaseous and aerosol content, can be continuously monitored. The homogeneity of the mixture is ensured by a fan placed at the bottom of the chamber which allows a mixing time of about 180 s, with a fan rotating speed of 1.6 revolutions per second. Between consecutive experiments, ChAMBRé can be evacuated to 10⁻⁵ mbar using a composite pumping system, which includes a TRIVAC® D65B rotary pump, a RUVAC WAU 251 root pump, and a Turbovac 1000, all from Leybold Vacuum. Before and during the experiments, ambient air enters the chamber through a five-stage filtering and purifying inlet, which includes a HEPA filter (model PFIHE842; NW25/40 inlet/outlet – 25/55 SCFM; 99.97% efficient at 0.3 μ m). The chamber is equipped with several flanges to allow a large panel of instruments to be connected to measure online and offline gaseous composition in addition to aerosol concentration and properties inside the volume: an overview of the

techniques used to characterize soot particles is reported in the following Sections. A detailed description of ChAMBRé can
95 be found in Massabò et al., 2018; Danelli et al., 2021, Vernocchi et al., 2023.

A total of 10 experiments were performed to investigate the properties of carbonaceous aerosols and observe the changes in
MAC by varying different fuel types and combustion conditions, as summarized in Table 1. Soot particles were introduced
into ChAMBRé, as detailed in Sect. 2.1, and were monitored using online instrumentation and sampled for offline analysis at
various time intervals to investigate the concentration of emitted particles, their size distribution, and optical properties. Both
100 optical and thermal-optical techniques were used for measurements. The combination of optical and thermal-optical analyses
offers several advantages, such as the ability to determine the MAC value (Janssen et al., 2011; Gentner et al., 2012; Robinson
et al., 2007) of the particulate matter in specific conditions and to improve the accuracy of OC/EC separation (Pio et al., 2011).

Table 1 Full list of the experiments analyzed in the present work. Additional information includes the start and total duration of the sampling and measurement interval for soot particles.

Date	Experiment	Type of Fuel – Soot particles source	Start of the experiment	Meas. Interval [min]
17/07/2024	P1a	Propane – MISG	3 min after the injection	110
17/07/2024	P1b	Propane – MISG	2 hours after the injection	190
18/07/2024	P2	Propane – MISG	3 min after the injection	120
19/07/2024	D3a	DIESEL - 65230 – 6 kW -Hyundai	3 min after the injection	120
19/07/2024	D3b	DIESEL - 65230 – 6 kW -Hyundai	2 hours and 30 minutes after the injection	110
22/07/2024	D4a	DIESEL - 65230 – 6 kW -Hyundai	3 min after the injection	190
22/07/2024	D4b	DIESEL - 65230 – 6 kW -Hyundai	4 hours after the injection	150
23/07/2024	H5a	HVO - 65230 – 6 kW -Hyundai	3 min after the injection	80
23/07/2024	H5b	HVO - 65230 – 6 kW -Hyundai	5 hours after the injection	130
24/07/2024	H6	HVO - 65230 – 6 kW -Hyundai	3 min after the injection	100
25/07/2024	H7a	HVO - 65230 – 6 kW -Hyundai	30 min after the injection	70
25/07/2024	H7b	HVO - 65230 – 6 kW -Hyundai	4 hours after the injection	130
26/07/2024	H8	HVO - 65230 – 6 kW -Hyundai	3 min after the injection	170
16/12/2024	P9a	Propane – MISG	3 min after the injection	60
16/12/2024	P9b	Propane – MISG	1 hour and 30 min after the injection	120
17/12/2024	P10a	Propane – MISG	3 min after the injection	60
17/12/2024	P10b	Propane – MISG	1 hour and 20 min. after the injection	180

2.1 Particle Generation

Injections of fresh soot particles inside ChAMBRé were performed by a mini-inverted soot generator (MISG; Argonaut Scientific Corp., Edmonton, AB, Canada; model MISG-2), fueled with propane and by a 12 HP 4-stroke diesel engine (Electrical Generator 65230 – 6 kW - Hyundai), fueled alternatively with regular fossil diesel and HVO. HVO is a renewable biofuel made by hydrotreating vegetable oils, animal fats or waste oils. It is considered environmentally friendly because it is free of aromatics, oxygen, and sulfur, and can potentially reduce emissions compared to conventional diesel (Zeman et al., 2019, Orlínski, P. et al., 2024). HVO meets diesel fuel standards, allowing it to be used in existing engines and infrastructure without modifications.

The MISG is an inverted-flame burner often considered as an ideal soot source, due to its capacity to generate almost pure EC particles (Stipe et al., 2005, Moallemi et al., 2019 and references therein). The MISG can be operated with different fuels, such

as ethylene (Kazemimanesh et al., 2019) and propane (Moallemi et al., 2019; Bischof et al., 2019). A comprehensive characterization of the MISG soot particles to perform experiments in atmospheric simulation chambers is reported in Vernocchi et al., 2022.

In this study, the MISG, considered as reference EC-dominated soot source, was fueled with propane with fixed air-to-fuel flow ratio, based on Vernocchi et al., 2022. Operative conditions selected for propane combustion are reported in Table 2. The efficiency of the combustion process (i.e. fuel lean/rich) can be expressed in terms of the global equivalence ratio (φ), which is the ratio of the actual fuel-to-air ratio to the stoichiometric fuel-to-air ratio, as follows:

$$\varphi = \frac{(m_F/m_A)}{(m_F/m_A)_{st}}, \quad (2)$$

where (m_F/m_A) and $(m_F/m_A)_{st}$ respectively are the actual and the stoichiometric fuel-to-air ratios. The fuel-to-air ratio is the inverse of the air-to-fuel ratio (AFR), which is the ratio of air to fuel mass. The stoichiometric AFR value for propane is 15.64 (inverse value is 0.064). In this work, only fuel-lean conditions were used with the MISG (i.e. $\varphi < 1$) considering that low fuel-to-air ratios are expected to produce particles with a high fraction of EC (Mamakos et al., 2013).

Diesel exhaust emissions were produced by the engine of the electrical generator and introduced into ChAMBRé using the same experimental layout adopted for the MISG and fully described in Vernocchi et al., 2022. The Hyundai Electrical Generator 65230 was connected to ChAMBRé using a connection line made with Swagelok Adaptors (size 3/4’’; 19.05) and ISO-K flanges (16 mm diameter) to prevent any possible leaks. The diesel generator is compliant with the Stage V EU normative, introduced in 2019 to reduce harmful pollutants like nitrogen oxides (NO_x) and particulate matter (PM) from diesel-powered equipment (Regulation EU 2016/1628). The generator, powered by a 12 HP, 4-stroke diesel engine, is designed to operate with standard diesel fuel. It was modified to allow connection to a second tank containing HVO. Between the use of different fuels, the system was properly heated to ensure there was no contamination or overlap of fuels in the production of soot particles. The injection of soot particles with the engine lasted only a few seconds to avoid exceeding the concentration of particles inside the chamber.

Table 2 Combustion parameters selected for MISG propane combustion.

Labels of experiments	Air Flow [L min ⁻¹]	Fuel Flow [mL min ⁻¹]	Global equivalent ratio
P1 – P2	10	80	0.200
P9 – P10	7	80	0.278

2.2 Experimental protocol

At the beginning of each experiment, soot particles were injected into ChAMBRé, and sampling began once the soot concentration stabilized. This typically occurs in approximately 3 minutes, corresponding to the chamber mixing time. Once

injected, the soot particles were left in suspension for defined timeframes and monitored with online instrumentation and sampled for offline analysis. In this study, all the experiments were performed at atmospheric pressure, $21\text{ }^{\circ}\text{C} < T < 25\text{ }^{\circ}\text{C}$,
145 RH<50 % and dark conditions.

2.3 Online optical aerosol measurements

One photoacoustic extinction meter (PAX) from Droplet Measurement Technologies was used to measure soot particles absorption coefficients at 870 nm. PAX has two measurement cells where aerosol optical properties are determined by light absorption and scattering. Soot particles absorb light and release acoustic waves detected by a microphone and the intensity of
150 the acoustic signal is interpreted to infer the particle absorption coefficient, while a wide-angle reciprocal nephelometer measures the scattering coefficient. No correction for truncation angle is applied, which can underestimate the scattering coefficient. However, since soot particles are generally smaller than $1\text{ }\mu\text{m}$ with SSA values below 0.3 (Moallemi et al., 2019), this issue was disregarded.

One Giano_BC1 from Dadolab srl, a PM_x sequential sampler with a built-in integrated Black Carbon optical monitor (Caponi
155 et al. 2022) was connected to ChAMBRé, allowing for the continuous monitoring of BC concentrations on filter during the PM sampling. After sampling and the PM gravimetric determination, the same filter can be used for the thermal-optical OC and EC quantification. Thus, the MAC value (see paragraph 2.5 for more details) used to calculate BC concentrations can be tuned to the specific composition of collected PM.

Data acquired during the experiments from different instruments were treated to homogenize their temporal resolution, in
160 particular PAX data were averaged over the same 15-minute intervals used by Giano_BC1.

2.4 Offline aerosol measurements

Soot particles were collected for offline analysis on pre-baked quartz fibre filters (25, 37, 47-mm diameter, Grade Quartz, Heat Treated Binderless Microfiber Filter, LabExact) using various low-volume samplers. The first one was the Giano_BC1, which
165 was directly connected to ChAMBRé, without its sampling head. To prevent rapid depletion of the chamber, considering the numerous samplers and monitors connected to ChAMBRé during the experiments, the sampler was operated at the fixed flow of 10 L min^{-1} .

Additionally, up to four Gilian GilAir Plus personal samplers were used in parallel with different size-selective inlets: IOM classifier for inhalable dust (up to 100 micrometers), two cyclones for respirable dust (up to 4 micrometers), and one personal impactor PEM-2-2.5 from TSI for particles less than 2.5 micrometers. These size-selective samplers adhere to health-based
170 conventions adopted by ISO and CEN to define particle size-selective occupational exposure limits (OELs) for aerosols. These OELs match the relevant sites of aerosol deposition in the respiratory tract and the associated health effects for exposure assessment. The four classifiers were directly inserted into the atmospheric chamber through a door flange located on one of the larger

flanges of the chamber central ring (Massabò et al. 2018). The samplers were secured inside the chamber using special hooks to keep them in the correct vertical position throughout the experiment (as if they were worn by an operator). The pumps were positioned outside the atmospheric chamber and connected to the dimensional selectors with specific tubes that passed through the door flange via small through-tube flanges. All sampling began simultaneously with flow rates ranging from 1.7 to 10 L min⁻¹ for 60 to 190 minutes (see Table 1). The operating conditions and flow rates used with the samplers are reported in Table 3.

Particle-loaded filters were firstly analyzed using the multi-wavelength absorbance analyzer (MWAA; Massabò et al., 2013, 2015), a laboratory instrument for the offline direct quantification of aerosol absorption coefficients (b_{abs}) at five different wavelengths (850, 635, 532, 405, and 375 nm). These features have been utilized in several field campaigns in urban and rural sites (Scerri et al., 2018; Massabò et al., 2019, 2020; Moschos et al., 2021) and in remote sites (Massabò et al., 2016; Saturno et al., 2017; Baccolo et al., 2020).

After MWAA measurements, the EC and OC mass concentrations were determined by thermal-optical transmittance analysis (TOT) using a Sunset Laboratory Inc. Sunset EC/OC analyzer and the NIOSH 5040 protocol (NIOSH, 2016). The NIOSH 5040 protocol is primarily intended for assessing workplace exposure to particulate diesel exhaust, but thermal-optical analysis is also routinely applied to environmental carbonaceous aerosols (EN 16909:2017, Brown et al., 2017).

Table 3 List of instruments and selectors used to collect aerosol particles during the experiments. Particle fraction collected, flow rate and filter diameter are also given.

Sampler	Classifier	Particle fraction collected	Flow rate [L min ⁻¹]	Filter diameter [mm]
Gilian GilAir Plus	Cyclone	Respirable fraction	1.7	25
Gilian GilAir Plus	Cyclone	Respirable fraction	1.7	37
Gilian GilAir Plus	IOM	Inhalable fraction	2	25
Gilian GilAir Plus	TSI PEM-2-2.5	PM _{2.5}	2	37
Giano BC1	None	Total	10	47

2.5 Retrieval of aerosol mass absorption cross section

The optical properties of the aerosol produced from each fuel were characterized by determining b_{abs} . The b_{abs} definition applies both to measurements directly performed on the aerosol dispersed in the atmosphere and to offline analysis on aerosol collected on filters, if appropriate data processing methods are applied (Massabò and Prati, 2021; and references therein). The b_{abs} values were calculated offline by the MWAA analysis on the sampled filters during each experiment (see Sect. 2.4) and online by Giano_BC1 and the PAX. This gave the possibility to compare different optical techniques on the same carbonaceous aerosol.

Offline MWAA analysis determined b_{abs} at 635 and 850 nm on the sampled filters (see Sect. 2.4). The b_{abs} values at 635 and 870 nm were derived also from online measurements throughout each experiment from Giano_BC1 measurements and PAX monitor, respectively.

The b_{abs} values thus derived at different wavelengths, along with the elemental carbon (EC) concentration measured on the filters (see sec. 2.4), were used to calculate the mass absorption coefficient (MAC) of the aerosol using the relation:

$$b_{abs} = MAC \times [EC] \quad (3)$$

where b_{abs} (Mm^{-1}) is the absorption coefficient, MAC ($m^2 g^{-1}$) is the mass absorption coefficient, and EC ($\mu g m^{-3}$) is the elemental carbon concentration.

2.6 Size distribution measurements

Particle concentration and size distribution inside the chamber were measured at 1-minute intervals using a scanning mobility particle sizer (SMPS 3938, TSI Inc.), equipped with a differential mobility analyzer (DMA 3081A) and a condensation particle counter (CPC 3750), operating at sheath/sample flow rates of 1.6/0.17 L min^{-1} . Measurements were corrected for diffusion losses using the instrument software. The SMPS was configured to measure particles with mobility diameters ranging from 18 to 806 nm.

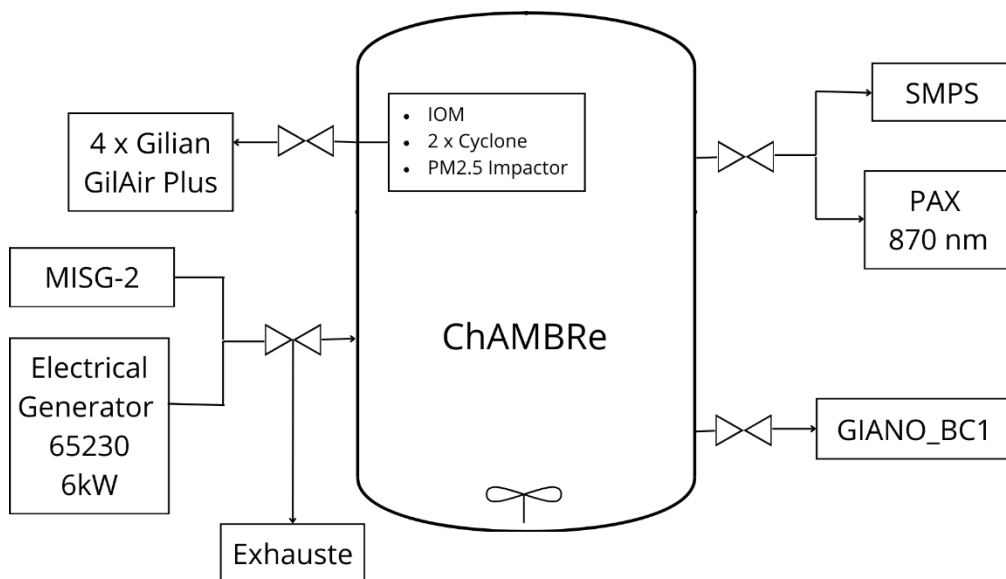


Figure 1 Simplified layout of the experimental setup at ChAMBRé. The setup includes a mini-inverted soot generator (MISG-2), an electrical generator diesel engine (Electrical Generator 65230 – 6 kW), a Scanning Mobility Particle Sizer (SMPS), a Photoacoustic Extinctionmeter (PAX) operating at 870 nm, a GIANO_BC1 sampler and up to four Gilian GilAir Plus personal samplers equipped

with different size-selective inlets (IOM classifier for inhalable dust, cyclones for respirable dust and a PM_{2.5} personal impactor for airborne particles less than 2.5 µm).

3. Results and discussion

3.1 EC/OC quantification

220 The EC/OC composition was quantified by thermal–optical analysis of samples collected on quartz fibre filters during each experiment. As shown in Figure 2, all the different types of size-selective samplers, which are designed to collect different size fractions of particulate matter to monitor worker exposure, showed comparable EC concentrations. This uniform efficiency across different samplers and fuels, whether diesel, HVO, or propane, highlights their reliability in accurately measuring ultrafine particles, confirming that these classifiers are suitable for assessing worker exposure to soot particles, 225 ensuring consistent and reliable data across various conditions and fuel types.

The EC:TC concentration ratio with propane resulted to be (0.7 ± 0.1) , in accordance with the results published in Vernocchi et al., 2022. The EC:TC concentration ratios were found to be $EC:TC = (0.15 \pm 0.05)$ and (0.4 ± 0.2) , for diesel and HVO, respectively. OC was the dominant fraction in all samples except for those from the soot generator, where EC was dominant. Several studies have indicated that EC is the dominant component in PM emissions from diesel vehicles (Chiang et al., 2012; 230 Grieshop et al., 2006; Kleeman et al., 2000), while other studies have reported contrasting results (Shah et al., 2004; Wu et al., 2016; Wang et al., 2021).

In Table 4 are summarized the average and standard deviation of EC:OC and EC:TC ratios obtained for each fuel type. In this study, a high proportion of OC was observed, summing up 60% to 85% of TC in both HVO and diesel cases. The EC:OC ratio value is influenced by factors like emission standards, engine power, maintenance, fuel's chemical composition, physical 235 properties, and experimental conditions (Lu et al., 2012; Zhang et al., 2009; Zhang et al., 2015). For example, Gali et al. 2017 indicated that under cold idle or low-engine-speed conditions, OC is the dominant fraction in particulate matter (PM), mainly originating from unburned fuel and incomplete combustion (Shah et al., 2004). Lower engine temperatures during idling performed in this case study can result in less complete combustion, which likely explains the high OC levels observed (Jung and Bae, 2015). This high proportion of OC could be attributed to factors like incomplete combustion and lower engine 240 temperatures during idling. Moreover, the heterogeneous effects of biodiesel on OC and EC may alter the composition of TC emissions (Williams et al., 2012; Agarwal et al., 2013). In addition, it should be noted that the determination of OC using a quartz filter can be affected by both positive and negative artifacts, such as volatilization losses and adsorption of vapor-phase organic compounds (Eatough et al. 1993, Appel et al., 1983).

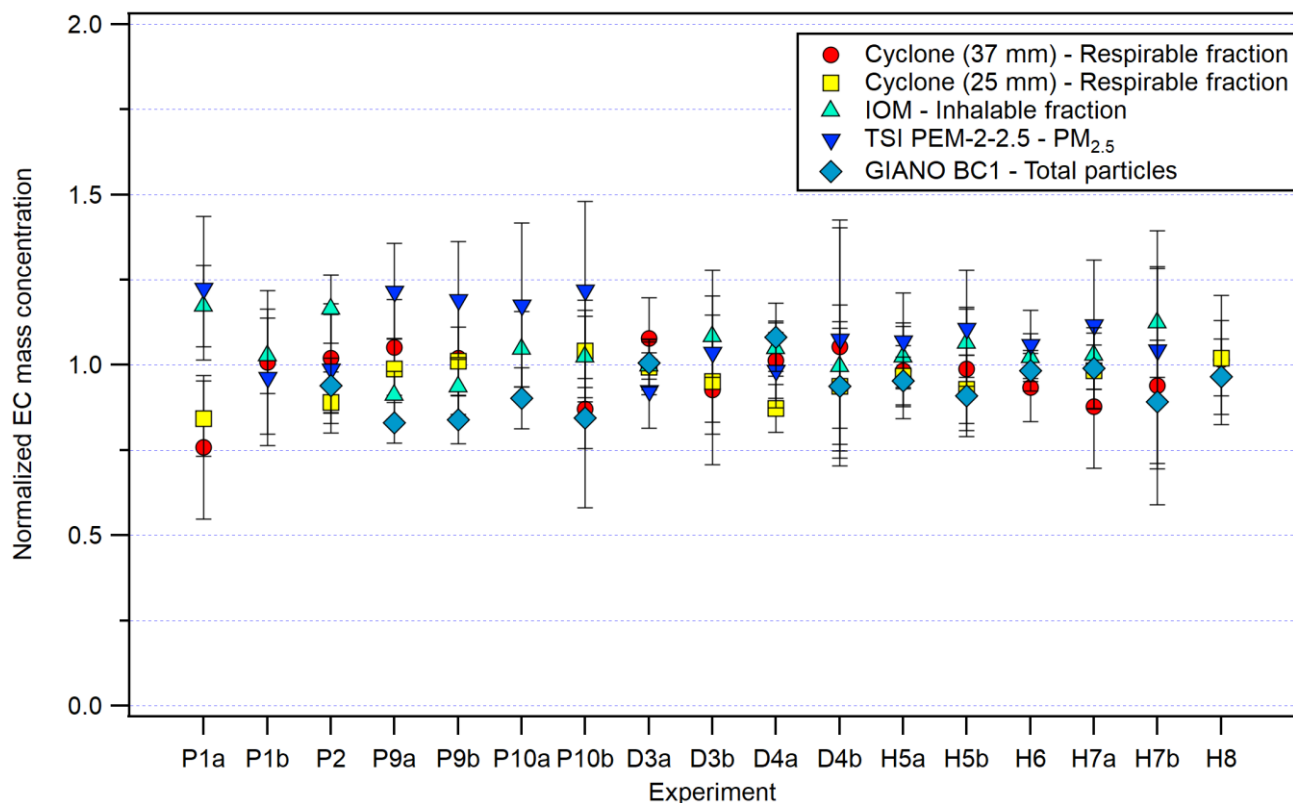


Figure 2 Normalized EC mass concentration across different experiments. All selectors operated simultaneously within the same time period. In order to help in the interpretation of data values have been normalized to a scaling factor equal to the mean value of each dataset (i.e. mean values of EC mass concentration retrieved from filters analysis during each experiment).

Table 4 Summary of the EC:OC and EC:TC ratio obtained for each fuel expressed as average value \pm one standard deviation.

	EC:OC	EC:TC
Propane – MISG	2.2 ± 0.8	0.7 ± 0.1
DIESEL - 65230 – 6 kW -Hyundai	0.2 ± 0.1	0.15 ± 0.05
HVO - 65230 – 6 kW -Hyundai	0.7 ± 0.5	0.4 ± 0.2

3.2 Size distribution measurements

A comparison of the size distributions of the generated aerosols for all fuels at the time of injection is presented in Figure 3. The data acquisition started 3 minutes after the end of injection of combustion aerosols; the data reported here are the average of the 4 consecutive minutes time interval. For fresh soot immediately after injection into ChAMBRe, the size distributions

255 for each fuel exhibit monomodal log-normal distributions. The MISG propane-soot aerosol shows a main peak between 200-300 nm, as expected (see Vernocchi et al., 2022). Regarding diesel exhaust emissions, particles from regular fossil diesel display a main peak roughly between 70 and 80 nm, while particles from HVO combustion show a slightly shifted peak at 80-90 nm.

The differences in the size distributions of aerosols generated from different fuels could be explained by the distinct combustion characteristics and chemical compositions of each fuel. For propane, the main peak between 200-300 nm is consistent with the combustion conditions (i.e. global equivalent ratio) used. The size distribution of the soot particles generated by the MISG is mainly affected by the global equivalence ratio, with a general trend suggesting that by decreasing air flow rate the mode diameter of generated particles increased (Vernocchi et al., 2022 and references therein).

In contrast, regular fossil diesel and HVO, which have a more complex hydrocarbon structure, tend to produce smaller particles. The main peak in the accumulation mode, consistent with literature data (Zhu et al., 2010, Chiavola O. et al., 2024, Böhmeke, C. et al., 2024), can be attributed to the incomplete combustion of heavier hydrocarbons, leading to the formation of smaller soot particles. Although here the two fuels show a similar size distributions, regular diesel generally emits more particles, with a size distribution shifted towards larger sizes compared to HVO. This is likely due to HVO's different chemical composition and aromatic-free nature, which may inhibit particle growth during combustion (Di Blasio et al., 2022). In combustion processes where EC predominates, such as in the case of propane used in this study, the emitted particulate matter typically exhibits the characteristic fractal-like structure of soot, which may affect the electric mobility diameter measured by the SMPS, resulting in greater values of mobility diameters. In contrast, when the soot OC fraction increases, the particle size tends to decrease, and the morphology shifts toward more compact, rounded aggregates (Heuser et al., 2024, Leskinen et al., 2023). Overall, literature indicates that results are highly dependent on engine architecture and loads, injection type, operating conditions, and specific fuel properties like viscosity, density and oxygen content (Böhmeke et al., 2024, Chiavola et al., 2024 and references therein). An accurate analysis of such aspects, however, goes beyond the scopes of the present stud

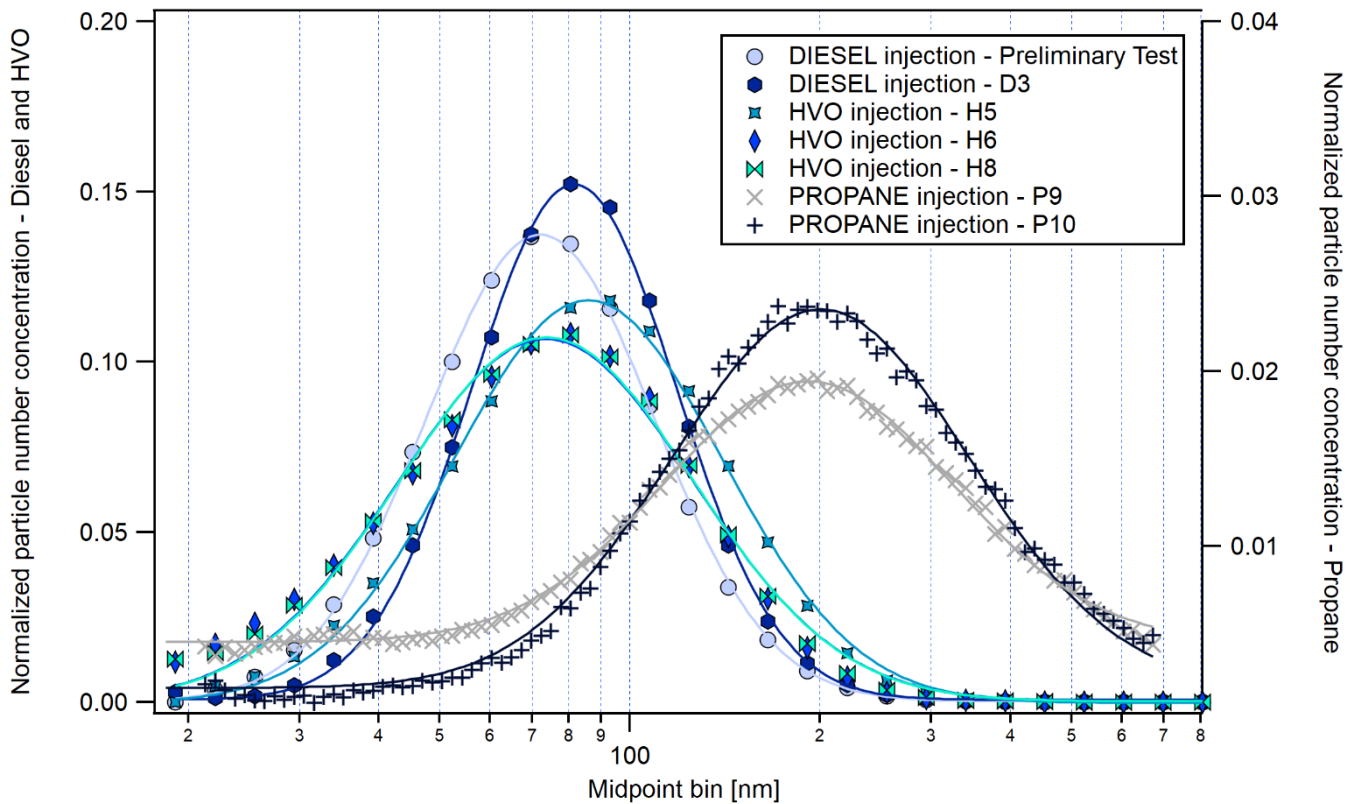


Figure 3 Number size distribution measured (markers) and fit extrapolated monomodal log-normal size distribution (lines) of generated aerosols just after the injection in ChAMBRe. Size data are normalized by the total number for each distribution.

3.3 Optical properties

The MAC values were calculated at 635 and 850/870 nm for each fuel, allowing the comparison at the same wavelength (nearly) between the filter-based technique (i.e. the MWAA, see Figure 4) and the b_{abs} retrieved online (at 635 nm from Giano_BC1 and at 870 nm from PAX). An average Ångström absorption exponent (AAE; Moosmüller et al., 2011) was calculated for each fuel by aggregating all available b_{abs} datasets from the MWAA analysis (Table 5). To facilitate the comparison with literature data, the MAC value at 550 nm was extrapolated from the MWAA measurement using the relation $MAC_{550} = MAC_{635} (635/550)^{AAE}$. All the measured MAC values are summarized in Table 6. The uncertainties were estimated from the fit uncertainty (statistical error based on the uncertainty of optical coefficients and mass concentration). At 635 nm, data indicates that the two techniques are generally consistent, except for the results for propane, where the two methods yielded significantly different MAC values. This discrepancy is likely due to the limited amount of data available for this fuel, which is also reflected in the larger error margin associated with the MAC value. At 850/870 nm MWAA and PAX measurements returned comparable MAC values for all the fuels. The results obtained with propane are in accordance with those previously reported by Vernocchi et al., 2022 and the extrapolated MAC value at 550 nm also aligns with literature data for pure BC (Bond and Bergstrom, 2006; Liu et al. 2020b).

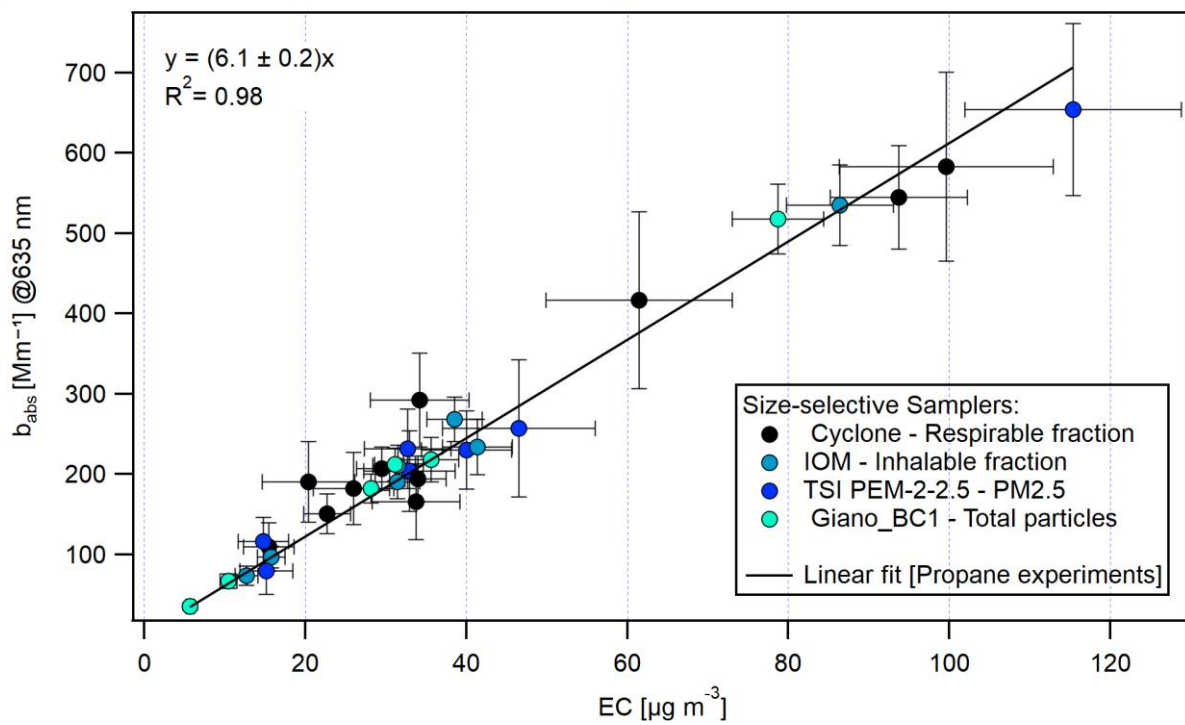
Table 5 AAE values obtained for propane, diesel and HVO through the analysis of MWAA raw data, expressed as average value \pm one standard deviation.

	Propane – MISG	DIESEL - 65230 – 6 kW -Hyundai	HVO - 65230 – 6 kW -Hyundai
Average AAE value	0.95 \pm 0.09	1.21 \pm 0.11	1.04 \pm 0.09

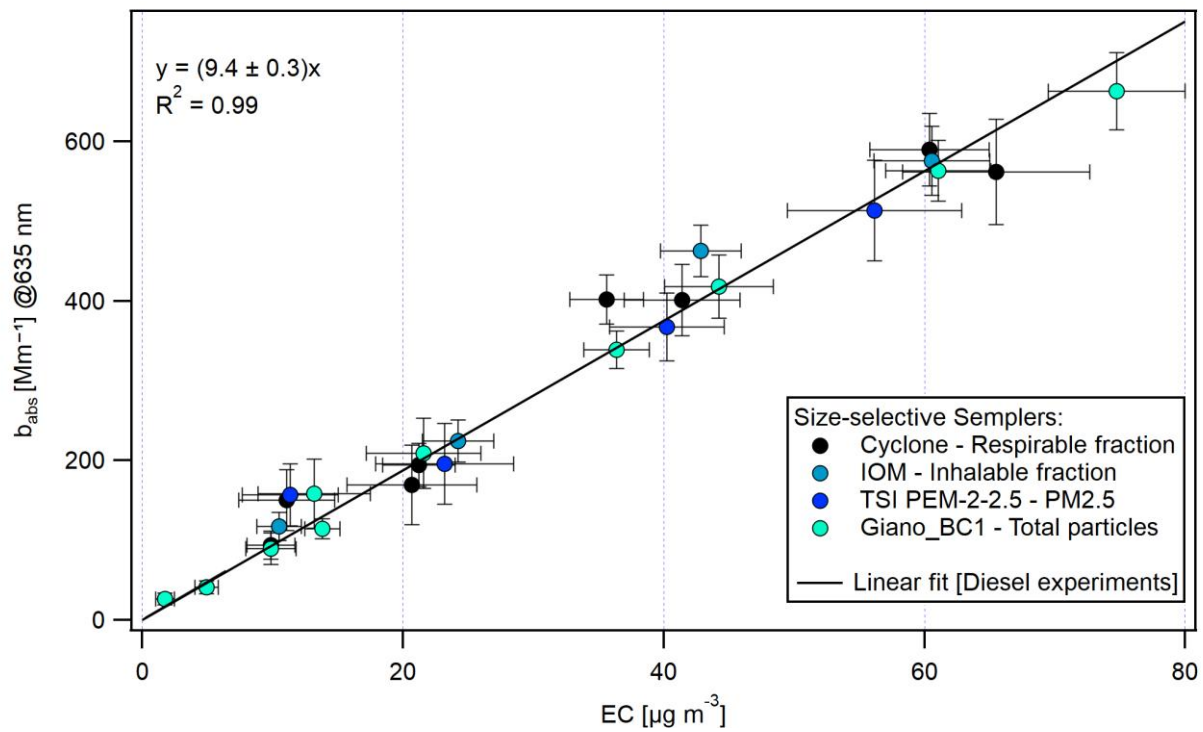
Table 6 Summary of the measured MAC values ($\text{m}^2 \text{g}^{-1}$).

	Propane – MISG	DIESEL - 65230 – 6 kW - Hyundai	HVO - 65230 – 6 kW - Hyundai
MAC values ($\text{m}^2 \text{g}^{-1}$) – MWAA 635 nm	6.1 \pm 0.2	9.4 \pm 0.3	8.0 \pm 0.3
MAC values ($\text{m}^2 \text{g}^{-1}$) – Giano BC1 635 nm	7.8 \pm 1.1	9.4 \pm 0.4	8.4 \pm 0.6
MAC values ($\text{m}^2 \text{g}^{-1}$) – MWAA 850 nm	5.2 \pm 0.5	6.8 \pm 0.2	6.0 \pm 0.3
MAC values ($\text{m}^2 \text{g}^{-1}$) – PAX 870 nm	5.5 \pm 0.1	6.2 \pm 0.5	5.8 \pm 0.2
Extrapolated MAC values ($\text{m}^2 \text{g}^{-1}$) – 550 nm	7.0 \pm 0.3	11.2 \pm 0.4	9.2 \pm 0.4

a)



b)



c)

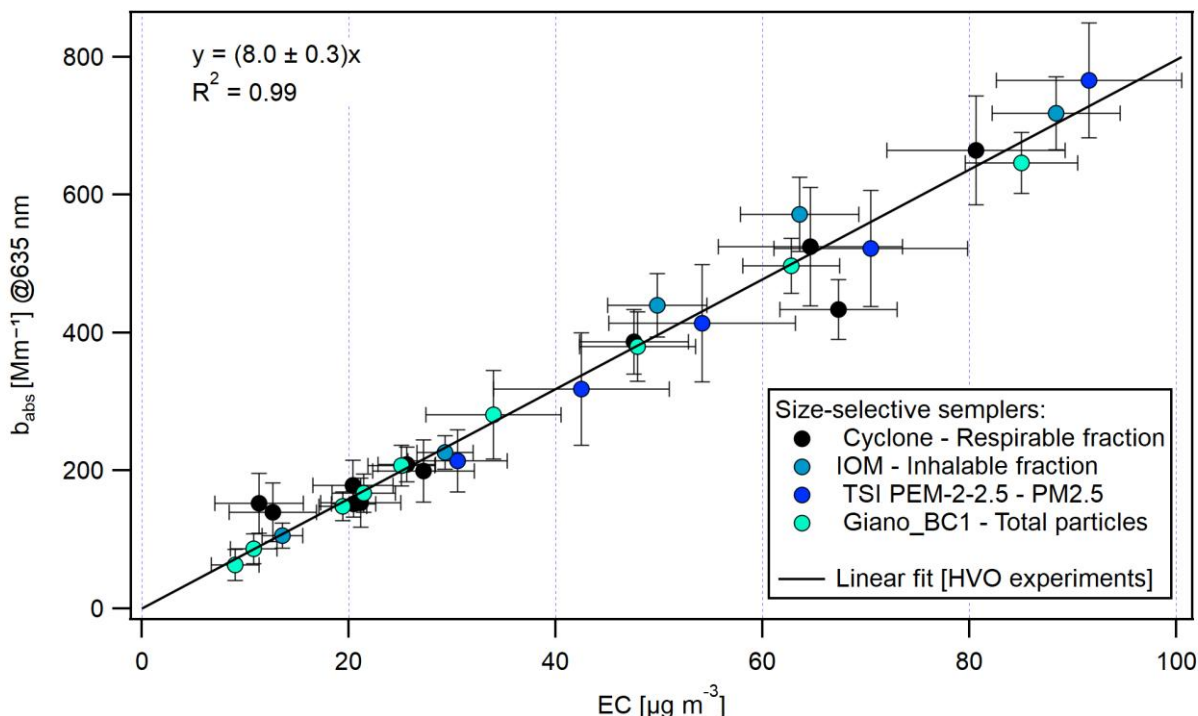


Figure 4 Absorption coefficient (b_{abs}) at 635 nm, measured by MWA vs. EC concentration ($\mu g m^{-3}$) for propane flame particles (a), commercial diesel exhaust particles (b) and HVO exhaust particles (c). For each classifier the corresponding particle size-selective sampling convention is also indicated. Linear fits (red lines) are plotted, with slopes representing the MAC values. The correlation coefficients (R^2) for each fit are also provided.

In general, the optical properties of the investigated aerosols, in terms of b_{abs} and MAC, revealed differences in absorption characteristics across different fuels: particles generated by diesel combustion were found to be more light absorbing than those produced by propane and HVO. MAC parameter values are higher for diesel, indicating more absorbent particulate matter, while HVO and propane show lower MAC values, even above 20%. This behavior is consistent with the EC:TC ratios shown in Table 4: the presence of OC coating soot particles enhances light absorption due to the lensing effect (Bond et al., 2006; Lack et al. 2010; Lefevre et al., 2018).

Previous studies in the literature have shown that optical properties, such as absorption, depend on various factors including composition, mixing state, aging, and size (Kirchstetter et al., 2004; Lewis et al., 2008; Lack et al., 2012; Lack and Langridge, 2013; Filep et al., 2013; Utry et al., 2013, Utry et al., 2014). Although the present study analyzed fresh soot particles, differences in composition can be expected, as the soot particles investigated in this study were generated by burning different fuels and through different combustion processes. This also resulted in differences in the size distribution of the particles produced (Figure 3), all of which can contribute to the variations observed in the MAC values.

4. Conclusions

320 The emissions of three different fuels combustion - propane, conventional fossil diesel, and Hydrotreated Vegetable Oil (HVO)- in terms of particle size distribution, optical properties, and EC/OC concentration in the engine exhaust emissions were investigated using an atmospheric simulation chamber (ChAMBRé). The objective of the study was to evaluate and compare different methods of sampling and analyzing carbonaceous aerosols as well as to characterize the variability in the optical properties of fresh combustion aerosols as a function of fuel type. Soot particles were generated using a mini-inverted soot generator fuelled with propane, as EC dominant soot source, and a diesel engine running on regular diesel and Hydrotreated Vegetable Oil (HVO).

325 Different types of size-selective samplers, designed to collect different size fractions of particulate matter for monitoring worker exposure, were tested, showing consistent EC concentrations across different fuels combustion (diesel, HVO, propane). These findings are highly relevant for occupational exposure monitoring, as they show that different size-selective samplers, whether targeting inhalable, respirable, or total fractions, consistently capture ultrafine soot particles across various fuels, including “green diesel” alternatives, which are increasingly adopted, especially in the transport and industrial sectors. This
330 is particularly important given the lack of clear regulatory guidance on particle size cut-offs for diesel exhaust sampling in workplace settings. The demonstrated uniformity in EC measurements confirms that current samplers are reliable for assessing soot exposure, regardless of the sampling convention adopted, helping to ensure consistent and representative data for health risk assessments.

The EC/OC ratios of freshly emitted aerosols varied significantly depending on the combustion fuel and process, and this
335 variability appears to be closely linked to changes in the particles' size distribution and optical behavior. EC-dominated soot was found in the propane emission, according to the fuel-lean condition adopted with the MSIG, while OC-rich combustion particles were observed with diesel and HVO combustion performed with the engine. These results were consistent with previous studies and highlighting once again the influence of several factors such as combustion condition (engine temperature, maintenance, efficiency of the combustion process) and fuel composition on these ratios.

340 Size distribution measurements provided insights into the particle size distributions for different fuels, showing monomodal log-normal distributions with peaks varying according to fuel type and combustion process. As indicated in previous studies, particle size is influenced by factors such as engine type and load, operating conditions, and fuel properties. In this study, fuel-lean propane combustion produced EC-rich particles with larger diameter in the range of 200-300 nm while diesel and HVO combustion generated smaller particles, with a main peak in the accumulation mode, consistent with the higher OC content
345 and the low-temperature engine's idle operation.

The observed variability in EC/OC ratios and particles size is accompanied by changes in the optical properties of the soot particles. Both the absorption coefficient (b_{abs}) and mass absorption coefficient (MAC) varied significantly depending on the type of fuel. Fresh particles generated by regular fossil diesel combustion were found to be more light absorbing than those produced by propane and HVO, exhibiting higher MAC values. The MAC values, measured at different wavelengths (850/870

350 and 635 nm), ranged from 6.2 ± 0.5 to 9.4 ± 0.4 m² g⁻¹ for commercial diesel, from 5.8 ± 0.2 to 8.4 ± 0.6 m² g⁻¹ for HVO, and from 5.2 ± 0.5 to 7.8 ± 1.1 m² g⁻¹ for propane. The extrapolated MAC at 550 nm turned out to be 7.0 ± 0.3 m² g⁻¹ for propane, 9.2 ± 0.4 m² g⁻¹ for HVO and 11.2 ± 0.4 m² g⁻¹ for diesel. Finally, it should be noted that different optical analyses performed yielded consistent results in nearly all cases.

In conclusion, the findings underscore the importance of considering several factors in the assessment of carbonaceous aerosols emissions and their optical behavior. The type of emission source (e.g. engine type), the chemical composition of the fuel, and the specific combustion condition (e.g. temperature, efficiency) influence the optical properties of the emitted particles. In particular, the variability of the mass absorption coefficient under different combustion scenarios highlights the importance of a deep characterization of such aspects.

Furthermore, instruments based on the measurements of optical properties, due to their ability to provide continuous and real-time data, represent one of the most promising techniques for monitoring carbonaceous aerosols in both ambient air and workplace environments. However, the significant differences in aerosol optical properties across combustion processes require an accurate source characterization in order to apply the most appropriate MAC values when interpreting data from optical instruments.

In this context, the presented results provide a valuable framework for describing the diversity of fresh soot emissions from different fuels.

Data availability

The dataset for this paper can be accessed at <https://data.mendeley.com/datasets/v6p5r5dmdy/1> (Danelli., 2025)

Author contribution

PB conceived the study. PB, SD, and LC designed the experiments and discussed the results. SD and LC conducted the experiments with contributions by VV, FM, MB and DM. LC performed the MWAA measurements. LC, MDC and MS performed the thermal–optical measurements. SD and LC performed the full data analysis under the supervision of PB and DM and with contributions from VV, MB and TI. FT and AP contributed to definition of experimental setup and data analysis procedure definition. SD, PB and PP wrote the manuscript. All authors reviewed and commented on the paper.

Competing interests

375 The authors declare that they have no conflict of interest.

Acknowledgements

The PM_TEN group would like to express its gratitude to the INFN technical staff affiliated with ChAMBRé for their valuable support.

Funding

380 This research has been supported by the CALIPSO project (Airborne Carbon: Limits, Impact, Protocols, and Operational Standards), funded by the Regional Program PR FESR 2021 – 2027 of the Liguria Region and the IR0000032–ITINERIS, Italian Integrated Environmental Research Infrastructures System (D.D. n. 130/2022 - CUP B53C22002150006) funded by the EU (Next Generation EU PNRR, Mission 4 “Education and Research”, Component 2 “From research to business”, Investment 3.1, “Fund for the realization of an integrated system of research and innovation infrastructures”). This study was
385 carried out within the RETURN Extended Partnership and received funding from the European Union Next-GenerationEU (National Recovery and Resilience Plan – NRRP, Mission 4, Component 2, Investment 1.3 – D.D. 1243 2/8/2022, PE0000005). This work was supported by the National Institute for Nuclear Physics (INFN) through the HARDLIFE experiments.

References

- Ackerman, A., Toon, O., Stevens, D., Heymsfield, A., Ramanathan, V., and Welton, E.: Reduction of tropical cloudiness by
390 soot, *Science*, 288, 1042–1047, doi: 10.1126/science.288.5468.1042, 2000.
- Agarwal, A. K., Gupta, T., Dixit, N., Shukla, P. C.: Assessment of toxic potential of primary and secondary particulates/aerosols from biodiesel vis-a-vis mineral diesel fuelled engine. *Inhalation Toxicol* 25, 325–32, 2013.
- Anenberg, S. C., Horowitz, L. W., Tong, D. Q., and West, J. J.: An estimate of the global burden of anthropogenic ozone and fine particulate matter on premature human mortality using atmospheric modelling, *Environ. Health Perspec.*, 118, 1189–95,
395 doi: 10.1289/ehp.0901220, 2010.
- Appel, B. R., Tokiwa, Y., Kothny, E. L.: Sampling of carbonaceous particles in the atmosphere. *Atmospheric Environment* 17(9), 1787–1796, 1983.
- Baccolo, G., Nastasi, M., Massabò, D., Clason, C., Di Mauro, B., Di Stefano, E., Łokas, E., Prati, P., Previtali, E., Takeuchi, N., Delmonte, B., and Maggi, V.: Artificial and natural radionuclides in cryoconite as tracers of supraglacial dynamics: Insights
400 from the Morteratsch glacier (Swiss Alps), *CATENA*, 191, 104577, doi: 10.1016/j.catena.2020.104577, 2020.
- Becker, K. H.: Overview on the Development of Chambers for the Study of Atmospheric Chemical Processes, in: *Environmental Simulation Chambers: Application to Atmospheric Chemical Processes*, edited by: Barnes I. and Rudzinski K. J., Springer, Amsterdam, 1–26, doi: 10.1007/1-4020-4232-9_1, 2006.

- Bischof, O. F., Weber, P., Bundke, U., Petzold, A., and Kiendler- Scharr, A.: Characterization of the Miniaturized Inverted
405 Flame Burner as a Combustion Source to Generate a Nanoparticle Calibration Aerosol, *Emission Contr. Sci. Technol.*, 6, 37–
46, doi: 10.1007/s40825-019-00147-w, 2019.
- Böhmeke, C., Wagner, U. & Koch, T. Influence of the air–fuel-ratio and fuel on the reactivity of diesel soot. *Automot. Engine
Technol.*, 9, 7, doi: 10.1007/s41104-024-00145-3, 2024
- Bond, T. C. and Bergstrom, R. W.: Light Absorption by Carbonaceous Particles: An Investigative Review, *Aerosol Sci.
410 Technol.*, 40, 27–67, doi: 10.1080/02786820500421521, 2006.
- Bond, T. C., Habib, G., and Bergstrom, R. W.: Limitations in the enhancement of visible light absorption due to mixing state,
J. Geophys. Res. Atmospheres, 111, 2006JD007315, doi:10.1029/2006JD007315, 2006.
- Bond, T. C., Doherty, S. J., Fahey, D. W., Forster, P. M., Bernsten, T., DeAngelo, B. J., Flanner, M. G., Ghan, S., Kärcher, B.,
Koch, D., Kinne, S., Kondo, Y., Quinn, P. K., Sarofim, M. C., Schultz, M. G., Schulz, M., Venkataraman, C., Zhang, H.,
415 Zhang, S., Bellouin, N., Guttikunda, S. K., Hopke, P. K., Jacobson, M. Z., Kaiser, J. W., Klimont, Z., Lohmann, U., Schwarz,
J. P., Shindell, D., Storelvmo, T., Warren, S. G., and Zender, C. S.: Bounding the role of black carbon in the climate system:
A scientific assessment, *J. Geophys. Res.-Atmos.*, 118, 5380–5552, doi: 10.1002/jgrd.50171, 2013.
- Brown, R. J., Beccaceci, S., Butterfield, D. M., Quincey, P. G., Harris, P. M., Maggos, T., ... & Karanasiou, A.: Standardisation
of a European measurement method for organic carbon and elemental carbon in ambient air: results of the field trial campaign
420 and the determination of a measurement uncertainty and working range. *Environmental Science: Processes & Impacts*, 19(10),
1249-1259, 2017.
- Caponi L., Cazzuli G.; Gargioni G.; Massabò D.; Brotto P., Prati P.: A New PM Sampler with a Built-In Black Carbon
Continuous Monitor. *Atmosphere*, 13, 299, doi: 10.3390/atmos13020299, 2022.
- Caponi, L., Formenti, P., Massabó, D., Di Biagio, C., Cazaunau, M., Pangui, E., Chevaillier, S., Landrot, G., Andreae, M. O.,
425 Kandler, K., Piketh, S., Saeed, T., Seibert, D., Williams, E., Balkanski, Y., Prati, P., and Doussin, J.-F.: Spectral- and size-
resolved mass absorption efficiency of mineral dust aerosols in the shortwave spectrum: a simulation chamber study, *Atmos.
Chem. Phys.*, 17, 7175–7191, doi: 10.5194/acp-17-7175-2017, 2017.
- Cassee, F. R., Héroux, M. E., Gerlofs-Nijland, M. E., and Kelly, F. J.: Particulate matter beyond mass: Recent health evidence
on the role of fractions, chemical constituents and sources of emission, *Inhal. Toxicol.*, 25, 802–812, doi:
430 10.3109/08958378.2013.850127, 2013.
- Cavalli, F.; Viana, M.; Yttri, K.E.; Genberg, J.; Putaud, J.P. Toward a standardised thermal-optical protocol for measuring
atmospheric organic and elemental carbon: The EUSAAR protocol. *Atmos. Meas. Tech.* 2010, 3, 79–89.
- Chiang, H.-L., Lai, Y.-M. & Chang, S.-Y., Pollutant constituents of exhaust emitted from light-duty diesel vehicles.
Atmospheric environment, 47, 399-406, 2012.
- 435 Chiavola O, Matijošius J, Palmieri F, Recco E. Engine and Emission Performance of Renewable Fuels in a Small Displacement
Turbocharged Diesel Engine. *Energies.*; 17(24)6443, doi: 10.3390/en17246443, 2024.

- Danelli, S. G., Brunoldi, M., Massabò, D., Parodi, F., Vernocchi, V., and Prati, P.: Comparative characterization of the performance of bio-aerosol nebulizers in connection with atmospheric simulation chambers, *Atmos. Meas. Tech.*, 14, 4461–4470, doi: 10.5194/amt-14-4461-2021, 2021.
- 440 Danelli, S. G.: Dataset for "Measurement report: Investigation of Optical Properties of Different Fuels Diesel Exhaust by an Atmospheric Simulation Chamber experiment", Mendeley Data, V1, doi: 10.17632/v6p5r5dmdy.1.
- Di Blasio G., Roberto Ianniello R., Carlo Beatrice C.: Hydrotreated vegetable oil as enabler for high-efficient and ultra-low emission vehicles in the view of 2030 targets, *Fuel*, 310, doi: 10.1016/j.fuel.2021.122206, 2022.
- Eatough, D. J., Wadsworth, A., Eatough, D. A., Crawford, J. W., Hansen, L. D., Lewis, E. A.: A multiple-system, multi-
445 channel diffusion denuder sampler for the determination of fine-particulate organic material in the atmosphere. *Atmospheric Environment* 27(8), 1213-1219, 1993.
- Filep, Á., Ajtai, T., Utry, N., Pintér, M. D., Nyilas, T., Takács, S., Máté, Z., Gelencsér, A., Hoffer, A., Schnaiter, M., Bozóki, Z., and Szabó, G.: Absorption spectrum of ambient aerosol and its correlation with size distribution in specific atmospheric conditions after a red mud accident, *Aerosol Air Qual. Res.*, 13, 49–59, 2013.
- 450 Finlayson-Pitts, B. J. and Pitts Jr., J. N.: Chemistry of the upper and lower atmosphere: Theory, experiments and applications, Academic Press, San Diego, CA, ISBN 978-0-12-257060-5, 2000.
- Gali, N. K., Yang, F., Cheung, C. S. & Ning, Z., A comparative analysis of chemical components and cell toxicity properties of solid and semi-volatile PM from diesel and biodiesel blend. *Journal of Aerosol Science*, 111, 51-64, 2017.
- Gan, W. Q., Koehoorn, M., Davies, H. W., Demers, P. A., Tamburic, L., and Brauer, M.: Long-term exposure to traffic-related
455 air pollution and the risk of coronary heart disease hospitalization and mortality, *Environ. Health Persp.*, 119, 501–507, doi: 10.1289/ehp.1002511, 2011.
- Genberg, J., Denier Van Der Gon, H. A. C., Simpson, D., Swietlicki, E., Areskoug, H., Beddows, D., Ceburnis, D., Fiebig, M., Hansson, H. C., Harrison, R. M., Jennings, S. G., Saarikoski, S., Spindler, G., Visschedijk, A. J. H., Wiedensohler, A., Yttri, K. E., and Bergström, R.: Light-absorbing carbon in Europe – measurement and modelling, with a focus on residential wood
460 combustion emissions, *Atmospheric Chem. Phys.*, 13, 8719–8738, doi: 10.5194/acp-13-8719-2013, 2013.
- Gentner, D.R.; Isaacman, G.; Worton, D.R.; Chan, A.W.H.; Dallmann, T.R.; Davis, L.; Liu, S.; Day, D.A.; Russell, L.M.; Wilson, K.R.; et al. Elucidating secondary organic aerosol from diesel and gasoline vehicles through detailed characterization of organic carbon emissions. *Proc. Natl. Acad. Sci. USA*, 109, 18318–18323, 2012.
- Giannoni, M.; Calzolari, G.; Chiari, M.; Cincinelli, A.; Lucarelli, F.; Martellini, T.; Nava, S. A comparison between thermal-
465 optical transmittance elemental carbon measured by different protocols in PM_{2.5} samples. *Sci. Total Environ.*, 571, 195–205, 2016.
- Grieshop, A. P., Lipsky, E. M., Pekney, N. J., Takahama, S. & Robinson, A. L., Fine particle emission factors from vehicles in a highway tunnel: Effects of fleet composition and season. *Atmospheric Environment*, 40, 287-298, 2006.
- Harrison, R. M., Beddows, D. C. S., Jones A. M., Calvo A., Alves C., and Pio C.: An evaluation of some issues regarding the
470 use of aethalometers to measure woodsmoke concentrations, *Atmos. Environ.*, 80, 540–548, 2013.

- Heuser, J., Di Biagio, C., Yon, J., Cazaunau, M., Bergé, A., Pangui, E., Zanatta, M., Renzi, L., Marinoni, A., Inomata, S., Yu, C., Bernardoni, V., Chevaillier, S., Ferry, D., Laj, P., Maillé, M., Massabò, D., Mazzei, F., Noyalet, G., Tanimoto, H., Temime-Roussel, B., Vecchi, R., Vernocchi, V., Formenti, P., Picquet-Varrault, B., and Doussin, J.-F.: Spectral optical properties of soot: laboratory investigation of propane flame particles and their link to composition, *EGUsphere* [preprint], doi: 10.5194/egusphere-2024-2381, 2024.
- Hu, D., Alfarra, M. R., Szpek, K., Langridge, J. M., Cotterell, M. I., Belcher, C., Rule, I., Liu, Z., Yu, C., Shao, Y., Voliotis, A., Du, M., Smith, B., Smallwood, G., Lobo, P., Liu, D., Haywood, J. M., Coe, H., and Allan, J. D.: Physical and chemical properties of black carbon and organic matter from different combustion and photochemical sources using aerodynamic aerosol classification, *Atmos. Chem. Phys.*, 21, 16161–16182, doi: 10.5194/acp-21-16161-2021, 2021.
- Janssen, N.A.H.; Hoek, G.; Simic-Lawson, M.; Fischer, P.; van Bree, L.; ten Brink, H.; Keuken, M.; Atkinson, R.W.; Anderson, H.R.; Brunekreef, B.; et al. Black carbon as an additional indicator of the adverse health effects of airborne particles compared with PM₁₀ and PM_{2.5}. *Environ. Health Perspect.*, 119, 1691–1699, 2011.
- Jung, Y. and Bae, C.: Immaturity of soot particles in exhaust gas for low temperature diesel combustion in a direct injection compression ignition engine, *Fuel*, 161, 312–322, doi:10.1016/j.fuel.2015.08.068, 2015.
- Kanakidou, M.; Seinfeld, J.H.; Pandis, S.N.; Barnes, I.; Dentener, F.J.; Facchini, M.C.; Van Dingenen, R.; Ervens, B.; Nenes, A.; Nielsen, C.J.; et al. Organic aerosol and global climate modelling: A review. *Atmos. Chem. Phys.*, 5, 1053–1123, 2005.
- Kanaya, Y.; Komazaki, Y.; Pochanart, P.; Liu, Y.; Akimoto, H.; Gao, J.; Wang, T.; Wang, Z. Mass concentrations of black carbon measured by four instruments in the middle of Central east China in June 2006. *Atmos. Chem. Phys.*, 8, 7637–7649, 2008.
- Kazemimanesh, M., Moallemi, A., Thomson, K., Smallwood, G., Lobo, P., and Olfert, J. S.: A novel miniature inverted-flame burner for the generation of soot nanoparticles, *Aerosol Sci. Tech.*, 53, 184–195, doi: 10.1080/02786826.2018.1556774, 2019.
- Kirchstetter, T. W., Novak, T., and Hobbs, P. V.: Evidence that the spectral dependence of light absorption by aerosols is affected by organic carbon, *J. Geophys. Res.*, 109, D21208, doi: 10.1029/2004JD004999, 2004.
- Kleeman, M. J., Schauer, J. J. & Cass, G. R., Size and composition distribution of fine particulate matter emitted from motor vehicles. *Environmental Science and Technology*, 34, 1132–1142, 2000.
- Kumar, N. K., Corbin, J. C., Bruns, E. A., Massabó, D., Slowik, J. G., Drinovec, L., Moćnik, G., Prati, P., Vlachou, A., Baltensperger, U., Gysel, M., El-Haddad, I., and Prévôt, A. S. H.: Production of particulate brown carbon during atmospheric aging of residential wood-burning emissions, *Atmos. Chem. Phys.*, 18, 17843–17861, doi: 10.5194/acp-18-17843-2018, 2018.
- Lack, D. A. and Cappa, C. D.: Impact of brown and clear carbon on light absorption enhancement, single scatter albedo and absorption wavelength dependence of black carbon, *Atmospheric Chem. Phys.*, 10, 4207–4220, doi:10.5194/acp10-4207-2010, 2010.
- Lack, D. A. and Langridge, J. M.: On the attribution of black and brown carbon light absorption using the Ångström exponent, *Atmos. Chem. Phys.*, 13, 10535–10543, doi: 10.5194/acp-13-10535-2013, 2013.

- Lack, D. A., Langridge, J. M., Bahreini, R., Cappa, C. D., Middlebrook, A. M., and Schwarz, J. P.: Brown carbon and internal mixing in biomass burning particles, *P. Natl. Acad. Sci. USA*, 109, 14802–14807, 2012.
- Lefevre, G., Yon, J., Liu, F., and Coppalle, A.: Spectrally resolved light extinction enhancement of coated soot particles, *Atmos. Environ.*, 186, 89–101, doi:10.1016/j.atmosenv.2018.05.029, 2018.
- Lelieveld, J., Evans, J. S., Fnais, M., Giannadaki, D., and Pozzer, A.: The contribution of outdoor air pollution sources to premature mortality on a global scale, *Nature* 525, 367–371, doi: 10.1038/nature15371, 2015.
- Leskinen, J., Hartikainen, A., Väättäin, S., Ihalainen, M., Virkkula, A., Mesceriakovas, A., Tiitta, P., Miettinen, M., Lamberg, H., Czech, H., Yli-Pirilä, P.: Photochemical Aging Induces Changes in the Effective Densities, Morphologies, and Optical Properties of Combustion Aerosol Particles. *Environ. Sci. Technol.* 57, 13, 5137–5148, 2023
- Lewis, K., Arnott, W. P., Moosmüller, H., and Wold, C. E.: Strong spectral variation of biomass smoke light absorption and single scattering albedo observed with a novel dual-wavelength photoacoustic instrument, *J. Geophys. Res.*, 113, D16203, doi: 10.1029/2007JD009699, 2008.
- Liu, F., Yon, J., Fuentes, A., Lobo, P., Smallwood, G. J., & Corbin, J. C.: Review of recent literature on the light absorption properties of black carbon: Refractive index, mass absorption cross section, and absorption function. *Aerosol Science and Technology*, 54(1), 33–51. doi: 10.1080/02786826.2019.1676878, 2019.
- Lu, T., Huang, Z., Cheung, C. S., Ma, J.: Size distribution of EC, OC and particle-phase PAHs emissions from a diesel engine fueled with three fuels. *Science of the Total Environment*, 438, 33–41, 2012.
- Mamakos, A., Khalek, I., Giannelli, R., and Spears, M.: Characterization of Combustion Aerosol Produced by a Mini-CAST and Treated in a Catalytic Stripper, *Aerosol Sci. Tech.*, 47, 927–936, <https://doi.org/10.1080/02786826.2013.802762>, 2013.
- Massabò, D. and Prati P.: An overview of optical and thermal methods for the characterization of carbonaceous aerosol, *Riv. Nuovo Cimento*, 44, 145–192, doi: 10.1007/s40766-021-00017-8, 2021.
- Massabò, D., Altomari, A., Vernocchi, V., and Prati, P.: Two wavelength thermal–optical determination of light-absorbing carbon in atmospheric aerosols, *Atmos. Meas. Tech.*, 12, 3173–3182, doi: 10.5194/amt-12-3173-2019, 2019.
- Massabò, D., Bernardoni, V., Bove, M., Brunengo, A., Cuccia, E., Piazzalunga, A., Prati, P., Valli, G., and Vecchi, R.: A multi-wavelength optical set-up for the characterization of carbonaceous particulate matter, *J. Aerosol Sci.*, 60, 34–46, doi: 10.1016/j.jaerosci.2013.02.006, 2013.
- Massabò, D., Caponi, L., Bernardoni, V., Bove, M. C., Brotto, P., Calzolari, G., Cassola, F., Chiari, M., Fedi, M. E., Fermo, P., Giannoni, M., Lucarelli, F., Nava, S., Piazzalunga, A., Valli, G., Vecchi, R., and Prati, P.: Multi-wavelength optical determination of black and brown carbon in atmospheric aerosols, *Atmos. Environ.*, 108, 1–12, 2015.
- Massabò, D., Caponi, L., Bove, M. C., and Prati, P.: Brown carbon and thermal-optical analysis: a correction based on optical multiwavelength apportionment of atmospheric aerosols, *Atmos. Environ.*, 125, 119–125, doi: 10.1016/j.atmosenv.2015.11.011, 2016.

- Massabò, D., Danelli, S. G., Brotto, P., Comite, A., Costa, C., Di Cesare, A., Doussin, J. F., Ferraro, F., Formenti, P., Gatta, E., Negretti, L., Oliva, M., Parodi, F., Vezzulli, L., and Prati, P.: ChAMBRé: a new atmospheric simulation chamber for aerosol modelling and bio-aerosol research, *Atmos. Meas. Tech.*, 11, 5885–5900, doi: 10.5194/amt-11-5885-2018, 2018.
- Massabò, D., Prati, P., Canepa, E., Bastianini, M., Van Eijk, A. M. J., Missamou, T., and Piazzola, J.: Characterization of carbonaceous aerosols over the Northern Adriatic Sea in the JERICO-NEXT project framework, *Atmos. Environ.*, 228, 117449, doi: 10.1016/j.atmosenv.2020.117449, 2020.
- Menon, S., Hansen, J., Nazarenko, L., and Luo, Y.: Climate effects of black carbon aerosols in China and India, *Science*, 297, 2250–2253, doi: 10.1126/science.1075159, 2002.
- Moallemi, A., Kazemimanesh, M., Corbin, J. C., Thomson, K., Smallwood, G., Olfert, J. S., and Lobo, P.: Characterization of black carbon particles generated by a propane-fueled miniature inverted soot generator, *J. Aerosol Sci.*, 135, 46–57, doi: 10.1016/j.jaerosci.2019.05.004, 2019.
- Moore, R. H., Ziemba, L. D., Dutcher, D., Beyersdorf, A. J., Chan, K., Crumeyrolle, S., Raymond, T. M., Thornhill, K. L., Winstead, E. L., and Anderson, B. E.: Mapping the Operation of the Miniature Combustion Aerosol Standard (Mini-CAST) Soot Generator, *Aerosol Sci. Tech.*, 48, 467–479, doi: 10.1080/02786826.2014.890694, 2014.
- Moosmüller, H., Chakrabarty, R. K., Ehlers, K. M., and Arnott, W. P.: Absorption Ångström coefficient, brown carbon, and aerosols: basic concepts, bulk matter, and spherical particles, *Atmos. Chem. Phys.*, 11, 1217–1225, doi: 10.5194/acp-11-1217-2011, 2011.
- Moschos, V., Gysel-Beer, M., Modini, R. L., Corbin, J. C., Massabò, D., Costa, C., Danelli, S. G., Vlachou, A., Daellenbach, K. R., Szidat, S., Prati, P., Prévôt, A. S. H., Baltensperger, U., and El Haddad, I.: Source-specific light absorption by carbonaceous components in the complex aerosol matrix from yearly filterbased measurements, *Atmos. Chem. Phys.*, 21, 12809–12833, doi: 10.5194/acp-21-12809-2021, 2021.
- Nordmann, S., Birmili, W., Weinhold, K., Müller, K., Spindler, G., and Wiedensohler, A.: Measurements of the mass absorption cross section of atmospheric soot particles using Raman spectroscopy, *J. Geophys. Res.-Atmos.*, 118, 12075–12085, doi: 10.1002/2013JD020021, 2013.
- Orliński, P.; Sikora, M.; Bednarski, M.; Gis, M. The Influence of Powering a Compression Ignition Engine with HVO Fuel on the Specific Emissions of Selected Toxic Exhaust Components. *Appl. Sci.*, 14, 5893, doi: 10.3390/app14135893, 2024
- Petzold, A., Ogren, J. A., Fiebig, M., Laj, P., Li, S.-M., Baltensperger, U., Holzer-Popp, T., Kinne, S., Pappalardo, G., Sugimoto, N., Wehrli, C., Wiedensohler, A., and Zhang, X.-Y.: Recommendations for reporting “black carbon” measurements, *Atmos. Chem. Phys.*, 13, 8365–8379, doi: 10.5194/acp-13-8365-2013, 2013.
- Pio, C.; Cerqueira, M.; Harrison, R.M.; Nunes, T.; Mirante, F.; Alves, C.; Oliveira, C.; Sanchez de la Campa, A.; Artinano, B.; Matos, M. OC/EC ratio observations in Europe: Re-thinking the approach for apportionment between primary and secondary organic carbon. *Atmos. Environ.*, 45, 6121–6132, 2011.
- Pope, C. A., Burnett, R. T., Thun, M. J., Calle, E. E., Krewski, D., Ito, K., and Thurston, G. D.: Lung Cancer, Cardiopulmonary Mortality, and Long-term Exposure to Fine Particulate Air Pollution, *J. Am. Med. Assoc.*, 287, 1132–1141, 2002.

- 570 Putaud, J.P.; Van Dingenen, R.; Alastuey, A.; Bauer, H.; Birmili, W.; Cyrus, J.; Flentje, H.; Fuzzi, S.; Gehrig, R.; Hansson, H.C.; et al. A European aerosol phenomenology-3: Physical and chemical characteristics of particulate matter from 60 rural, urban, and kerbside sites across Europe. *Atmos. Environ.*, 44, 1308–1320, 2010.
- Quinn, P. K., Bates, T. S., Baum, E., Doubleday, N., Fiore, A. M., Flanner, M., Fridlind, A., Garrett, T. J., Koch, D., Menon, S., Shindell, D., Stohl, A., and Warren, S. G.: Shortlived pollutants in the Arctic: their climate impact and possible mitigation strategies, *Atmos. Chem. Phys.*, 8, 1723–1735, doi: 10.5194/acp-8-1723-2008, 2008.
- 575 Ramanathan, V. and Carmichael, G.: Global and regional climate changes due to black carbon, *Nat. Geosci.*, 1, 221–227, doi: 10.1038/ngeo156, 2008.
- Reisinger, P.; Wonaschütz, A.; Hitzenberger, R.; Petzold, A.; Bauer, H.; Jankowski, N.; Puxbaum, H.; Chi, X.; Maenhaut, W. Intercomparison of measurement techniques for black or elemental carbon under urban background conditions in wintertime: Influence of biomass combustion. *Environ. Sci. Technol.*, 42, 884–889, 2008.
- 580 Robinson, A.L.; Donahue, N.M.; Shrivastava, M.K.; Weitkamp, E.A.; Sage, A.M.; Grieshop, A.P.; Lane, T.E.; Pierce, J.R.; Pandis, S.N. Rethinking organic aerosols: Semivolatile emissions and photochemical aging. *Science*, 315, 1259–1262, 2007.
- Salako, G.O.; Hopke, P.K.; Cohen, D.D.; Begum, B.A.; Biswas, S.K.; Pandit, G.G.; Chung, Y.; Rahman, S.A.; Hamzah, M.S.; Davy, P.; et al. Exploring the Variation between EC and BC in a Variety of Locations. *Aerosol Air Qual. Res.*, 12, 1–7, 2012.
- 585 Sandrini, S.; Fuzzi, S.; Piazzalunga, A.; Prati, P.; Bonasoni, P.; Cavalli, F.; Bove, M.C.; Calvello, M.; Cappelletti, D.; Colombi, C.; et al. Spatial and seasonal variability of carbonaceous aerosol across Italy. *Atmos. Environ.*, 99, 587–598, 2014.
- Saturno, J., Pöhlker, C., Massabò, D., Brito, J., Carbone, S., Cheng, Y., Chi, X., Ditas, F., Hrabě de Angelis, I., Morán-Zuloaga, D., Pöhlker, M. L., Rizzo, L. V., Walter, D., Wang, Q., Artaxo, P., Prati, P., and Andreae, M. O.: Comparison of different Aethalometer correction schemes and a reference multiwavelength absorption technique for ambient aerosol data, *Atmos. Meas. Tech.*, 10, 2837–2850, doi: 10.5194/amt-10-2837-2017, 2017.
- 590 Scerri, M. M., Kandler, K., Weinbruch, S., Yubero, E., Galindo N., Prati, P., Caponi, L., and Massabò, D.: Estimation of the contributions of the sources driving PM_{2.5} levels in a Central Mediterranean coastal town, *Chemosphere*, 211, 465–481, doi: 10.1016/j.chemosphere.2018.07.104, 2018.
- Shah, S. D., Cocker, D. R., Miller, J. W., Norbeck, J. M.: Emission rates of particulate matter and elemental and organic carbon from in-use diesel engines. *Environmental Science & Technology* 38(9), 2544-2550, 2004.
- 595 Utry, N., Ajtai, T., Filep, Á., Dániel P. M., Hoffer, A., Bozoki, Z., and Szabó, G.: Mass specific optical absorption coefficient of HULIS aerosol measured by a four-wavelength photoacoustic spectrometer at NIR, VIS and UV wavelengths, *Atmos. Environ.*, 69, 321–324, 2013.
- Utry, N., Ajtai, T., Filep, Á., Pintér, M., Török, Z., Bozoki, Z., and Szabó, G.: Correlations between absorption Angström exponent (AAE) of wintertime ambient urban aerosol and its physical and chemical properties, *Atmos. Environ.*, 91, 52–59, 2014.
- 600

- Vernocchi, V., Brunoldi, M., Danelli, S. G., Parodi, F., Prati, P., Massabò, D.: Characterization of soot produced by the mini-inverted soot generator with an atmospheric simulation chamber, *Atmos. Meas. Tech.*, 15, 2159–2175, doi:10.5194/amt-15-2159-2022, 2022.
- 605 Vernocchi, V., Abd El, E., Brunoldi, M., Danelli, S. G., Gatta, E., Isolabella, T., Mazzei, F., Parodi, F., Prati, P., and Massabò, D.: Airborne bacteria viability and air quality: a protocol to quantitatively investigate the possible correlation by an atmospheric simulation chamber, *Atmos. Meas. Tech.*, 16, 5479–5493, doi: 10.5194/amt-16-5479-2023, 2023.
- Wang B., Lau Y-S., Huang Y., Organ B., Chuang H-C., Hang Ho S. S., Qu L., Lee S-C., Ho K-F., Chemical and toxicological characterization of particulate emissions from diesel vehicles, *Journal of Hazardous Materials*, Volume 405, 124613, ISSN 0304-3894, doi: 10.1016/j.jhazmat.2020.124613, 2021.
- 610 Weijers, E. P., Schaap, M., Nguyen, L., Matthijsen, J., Denier van der Gon, H. A. C., ten Brink, H. M., and Hoogerbrugge, R.: Anthropogenic and natural constituents in particulate matter in the Netherlands, *Atmos. Chem. Phys.*, 11, 2281–2294, doi: 10.5194/acp-11-2281-2011, 2011.
- Williams, A., McCormick, R. L., Hayes, R. R., Ireland, J., Fang, H. L.: Effect of 530 biodiesel blends on diesel particulate filter performance. SAE Technical Paper 2012-01-1666, 2012.
- 615 Wu, B., Shen, X., Cao, X., Yao, Z. & Wu, Y., Characterization of the chemical composition of PM_{2.5} emitted from on-road China III and China IV diesel trucks in Beijing, China. *Science of The Total Environment*, 551-552, 579-589, 2016.
- Zanatta, M., Gysel, M., Bukowiecki, N., Müller, T., Weingartner, E., Areskoug, H., Fiebig, M., 1115 Yttri, K. E., Mihalopoulos, N., Kouvarakis, G., Beddows, D., Harrison, R. M., Cavalli, F., Putaud, J. P., Spindler, G., Wiedensohler, A., Alastuey, A., Pandolfi, M., Sellegri, K., Swietlicki, E., Jaffrezo, J. L., Baltensperger, U., and Laj, P.: A European aerosol phenomenology-5: Climatology of black carbon optical properties at 9 regional background sites across Europe, *Atmos. Environ.*, 145, 346–364, doi: 10.1016/j.atmosenv.2016.09.035, 2016.
- Zeman P, Hönig V, Kotek M, Táborský J, Obergruber M, Mařík J et al. Hydrotreated vegetable oil as a fuel from waste materials. *Catalysts*; 9(4):337. doi: 10.3390/catal9040337, 2019.
- 625 Zhang, H., Magara-Gomez, K. T., Olson, M. R., Okuda, T., Walz, K. A., Schauer, J. J., 535 Kleeman, M. J.: Atmospheric impacts of black carbon emission reductions through the 536 strategic use of biodiesel in California. *Science of the Total Environment* 538, 412-422. 537, 2015.
- Zhu, L., Cheung, C. S., Zhang, W. G. and Huang, Z.: Influence of Methanol-Biodiesel Blends on the Particulate Emissions of a Direct Injection Diesel Engine', *Aerosol Science and Technology*, 44: 5, 362 - 369, doi: 10.1080/02786821003652646, 2010.
- 630